Dependency of Head Impact Rotation on Head-Neck Positioning and Soft Tissue Forces

Michael Fanton, Calvin Kuo, Jake Sganga, Fidel Hernandez, and David B. Camarillo, *Member, IEEE*

Abstract*—*Objective: **Humans are susceptible to traumatic brain injuries from rapid head rotations that shear and stretch the brain tissue. Conversely, animals such as woodpeckers intentionally undergo repetitive head impacts without apparent injury. Here, we represent the head as the end effector of a rigid linkage cervical spine model to quantify how head angular accelerations are affected by the linkage positioning (head-neck configuration) and the soft tissue properties (muscles, ligaments, tendons).** ***Methods:*** **We developed a two-pivot manipulator model of the human cervical spine with passive torque elements to represent soft tissue forces. Passive torque parameters were fit against five human subjects undergoing mild laboratory head impacts with tensed and relaxed neck muscle activations. With this representation, we compared the effects of the linkage configuration dependent end-effector inertial properties and the soft tissue resistive forces on head impact rotation.** ***Results:*** **Small changes in cervical spine positioning ($<$5 degrees) can drastically affect the resulting rotational head accelerations ($>$100%) following an impact by altering the effective end-effector inertia. Comparatively, adjusting the soft tissue torque elements from relaxed to tensed muscle activations had a smaller ($<$30%) effect on maximum rotational head accelerations. Extending our analysis to a woodpecker rigid linkage model, we postulate that woodpeckers experience relatively minimal head impact rotation due to the configuration of their skeletal anatomy.** ***Conclusion:*** **Cervical spine positioning dictates the head angular acceleration following an impact, rather than the soft tissue torque elements.** ***Significance:*** **This analysis quantifies the importance of head positioning prior to impact, and may help us to explain why other species are naturally more resilient to head impacts than humans.**

***Index Terms*—Musculoskeletal biomechanics, concussion, manipulator dynamics, injury biomechanics.**

Manuscript received April 2, 2018; revised June 13, 2018 and July 18, 2018; accepted August 10, 2018. Date of publication August 20, 2018; date of current version March 19, 2019. This work was supported in part by the Stanford University Child Health Research Institute, in part by the Stanford Bio-X Fellowship Program, in part by the Office of Naval Research Young Investigator Program (N00014-16-1-2949), and in part by the NSF Graduate Research Fellowship Program. *(Corresponding author: Michael Fanton.)*

M. Fanton is with the Department of Mechanical Engineering, Stanford University, Stanford, CA 94305 USA (e-mail: mfanton@stanford.edu).

C. Kuo and F. Hernandez are with the Department of Mechanical Engineering, Stanford University.

J. Sganga and D. B. Camarillo are with the Department of Bioengineering, Stanford University.

Digital Object Identifier 10.1109/TBME.2018.2866147

I. Introduction

BIOMECHANISTS and roboticists commonly model musculoskeletal systems as rigid-link manipulators to simplify control problems and understand dynamical properties [1], [2]. Analogous to rigid linkage robotic manipulators, many animals use their head to manipulate or interact with the environment, as the "end-effector" of their cervical spine. For example, the woodpecker repetitively drums its beak into tree bark, often at accelerations over 1000 g [3], to forage for food. Likewise, horned rams fight by butting heads at speeds of up to 15 m/s [4]. Humans too use their head like an end-effector, most commonly in contact sports such as American football where head-first tackles and blocks are quite common. However, more so than other species, humans are highly vulnerable to traumatic brain injuries (TBI), which can lead to debilitating diseases and chronic neurodegeneration [5].

Although the precise internal mechanisms of TBI in humans remain debated, it has been long hypothesized that head rotations can cause shearing and stretching of the brain tissue, and are strongly linked to mild TBI (mTBI). First proposed in the 1940's [6], there have been a number of studies confirming this notion [7]–[9]. As a mechanical linkage between the head and the torso, the cervical spine acts as a constraint on the head, governing its rotation and providing stabilizing forces during external perturbations. A prominent emerging theory in the field of human head impact biomechanics is that the soft tissue loads of the neck may act to reduce risk of mTBI [10]. Specifically, the effective stiffness and viscosity of the cervical spine has been strongly correlated to both muscle strength and activation level [11], [12], and these resistive forces may act to stabilize the head during impact.

While the benefits of neck stiffening are intuitively plausible, human subject studies evaluating its protective effects on the brain have yielded mixed results. The strongest clinical evidence linking neck strength to TBI is a prospective study which found a modest negative correlation between neck strength and concussion in a large group of high school athletes [13]. Laboratory human subject studies of sub-concussive head kinematics have found increased muscle activation and strength lowered head velocities in mild impact conditions [12], [14], [15]. Increased neck stiffness has also been found to significantly improve dynamic head stabilization during in-vivo impacts in controlled rugby tackles and soccer headers [16], [17].

Despite these findings, the negative correlation between neck stiffness and the peak angular velocity or acceleration

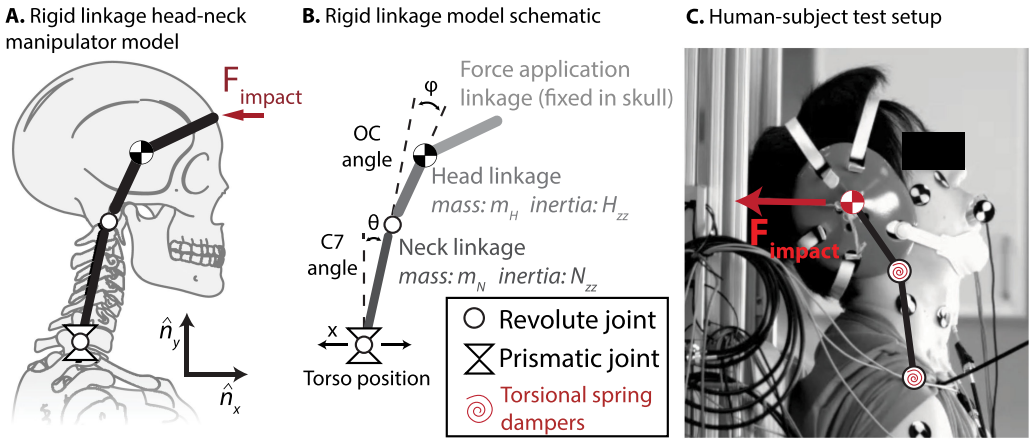

Fig. 1. Study overview. (a) To investigate how the cervical spine properties dictate head rotation in sagittal head impacts, we created a rigid linkage model of the human head and neck. The Newtonian reference frame $\hat{n}_x$, $\hat{n}_y$, $\hat{n}_z$ is shown. (b) The hard skeletal tissue was modeled as two rigid linkages, and the soft tissue modeled as passive torsional spring-dampers. A third linkage, fixed in the skull, connected between the head center of mass to the point of impact. (c) Spring and damper values were fit to human data of subjects undergoing mild head loading to induce sagittal extension.

experienced during a head impact has not been universally observed. In a variety of sports, athletes undergoing targeted cervical spine strength training did not increase head stabilization during field impacts, despite significantly stronger musculature post-training [18], [19]. In fact, it was found that hockey and football players with stronger neck muscles had equal odds of sustaining severe head accelerations compared to those with weaker muscles on the field [11], [20]. Impact awareness has been found to have no effect on head kinematics, and simulation results have also been inconclusive, with different rigid-body and finite element simulations disagreeing on the role of the neck in preventing mTBI [21]–[23].

Though less widely investigated, the positioning of the head, controlled by the cervical spine, also affects head rotation and injury risk. "Spearing" in American football is a situation in which striking player tackles an opponent using the crown of the helmet with his head, neck, and torso aligned. Although spearing is associated with a higher cervical spine injury risk [24], a study of 27 National Football League (NFL) impacts found that striking player experienced significantly lower head accelerations than the struck player; the authors attributed this to an increase in effective inertia by the striking player [25]. Although this study provided clinical evidence, the effect of cervical spine positioning on head inertial properties and resulting accelerations has yet to be quantified in a wide variety of head-neck configurations.

Motivated by conflicting results in previous studies on the role of the cervical spine in TBI, our goal was to comparatively and quantitatively investigate the relative effect of the head-neck positioning and soft tissue forces on head impact rotation in the sagittal plane. Both of these properties are easily modifiable by an individual and have been widely hypothesized to contribute to head rotation and TBI risk. By reducing the complexity of the head and neck system into a simplified rigid linkage model, we can draw on techniques from the field of robotics to gain global observations and analytical relationships on the effective head inertia and its rotational response to an input force. Using this methodology, we postulate that other species, such as the woodpecker, may have adapted specific cervical spine skeletal configurations that minimize head rotations.

II. Methods and Results

A. Rigid Linkage Head-Neck Model

The human neck is made up of seven cervical vertebrae that reside between the base of the skull and the thoracic vertebrae of the torso. Although sagittal plane bending of the neck is distributed throughout all seven vertebrae, many previous studies simplify the cervical spine into single, dual, or multi-joint models connected by rigid linkages [26]. In previous work [27], the authors experimentally found that the human cervical spine has complex motion in sagittal extension, with the instantaneous center of rotation greatly varying in height throughout an impact. Thus, a two-pivot model was chosen to represent the cervical spine, with a pin joint at the top of the neck to represent the occipital condyles (OC) of the atlanto-occipital joint, and a second pin joint at the C7 vertebra to represent bending of the lower neck (Fig. 1(a), (b)). To model soft tissue elastic and viscoelastic bending forces, torsional spring-dampers were located at each joint. The head, neck, and torso were treated as three separate rigid bodies. Link lengths were taken as the average 50% male values [28]. The torso was constrained as a prismatic slider joint to allow a horizontal translational degree of freedom to model small torso movements.

The dynamical system of equations that govern this head-neck linkage model are as follows, with parameters listed in Table I.

$$M \begin{bmatrix} \ddot{\theta} \\ \ddot{\phi} \\ \ddot{x} \end{bmatrix} + C = \begin{bmatrix} \sum M_{C7} \\ \sum M_{OC} \\ F_x \end{bmatrix} \tag{1}$$

TABLE I
HUMAN LINKAGE MODEL SYMBOLS AND PARAMETER VALUES

Symbol	Quantity	Value	Source
m_H	Head mass	4.0 kg	[28]
m_B	Body mass	100 kg	Estimated
m_N	Neck mass	1.2 kg	[28]
k_{C7}	C7 joint stiffness	See Table 2	Experimental fit
k_{OC}	OC joint stiffness	See Table 2	Experimental fit
ζ_{C7}	C7 joint damping	See Table 2	Experimental fit
ζ_{OC}	OC joint damping	See Table 2	Experimental fit
L	Lower linkage length	0.12 m	Estimated
h	Upper linkage length	0.06 m	[28]
H_{zz}	Head moment of inertia	0.025 kgm^2	[28]
N_{zz}	Neck moment of inertia	0.003 kgm^2	Estimated
x	Horizontal torso position	Variable	N/A
θ	C7 joint angle	Variable	N/A
φ	OC joint angle	Variable	N/A

The mass matrix M is derived as follows:

$$M_1 = \begin{bmatrix} H_{zz} + N_{zz} + m_H\left(h^2 + L^2 + 2hL\cos(\phi)\right) + \frac{1}{4}m_N L^2 \\ H_{zz} + m_H h^2 + m_H hL\cos(\phi) \\ -m_H\left(L\cos(\phi) + h\cos(\phi+\theta)\right) - \frac{1}{2}Lm_N\cos(\theta) \end{bmatrix}$$

$$M_2 = \begin{bmatrix} H_{zz} + m_H h^2 + m_H hL\cos(\phi) \\ H_{zz} + m_H h^2 \\ -m_H h\cos(\phi+\theta) \end{bmatrix}$$

$$M_3 = \begin{bmatrix} -m_H\left(L\cos(\phi) + h\cos(\phi+\theta)\right) - \frac{1}{2}Lm_N\cos(\theta) \\ -m_H h\cos(\phi+\theta) \\ m_H + m_B + m_N \end{bmatrix}$$

$$M = \begin{bmatrix} M_1 & M_2 & M_3 \end{bmatrix} \tag{2}$$

Matrix C contains the Coriolis and centrifugal terms:

$$C = \begin{bmatrix} m_H hL\sin(\phi)\left(\dot{\theta}^2 - \left(\dot{\phi} + \dot{\theta}\right)^2\right) \\ m_H hL\sin(\phi)\dot{\theta}^2 \\ m_H h\sin(\phi+\theta)\left(\dot{\phi} - \dot{\theta}\right)^2 + \frac{1}{2}\left(m_N + 2m_H\right)\dot{\theta}^2\sin\theta \end{bmatrix} \tag{3}$$

The matrix on the right side of Equation 1 contains the forces and moments on the system from the impact force, the neck joint torsional spring dampers, and gravity.

$$\sum M_{C7} = (r_{P/C7} \times F)\cdot\hat{n}_z + \tau_{C7} + g_{C7} \tag{4}$$

$$\sum M_{OC} = (r_{P/OC} \times F)\cdot\hat{n}_z + \tau_{OC} + g_{OC} \tag{5}$$

$F = [F_x\ F_y]$ represents the impact force on the system. $r_{P/C7}$ and $r_{P/OC}$ are the vectors from the impact point to the C7 and OC joints. τ_{C7} and τ_{OC} are the torque from the neck joint torsional spring dampers at the C7 and OC joints. g_{C7} and g_{OC} are the moments on the system due to gravity about the C7 and OC joints.

B. Human Subject Testing

To fit proper stiffness and damping at each torsional joints, human subject data of mild laboratory head impacts from a previous study were utilized [27]. In this study, five male subjects were recruited under Stanford Institutional Review Board (IRB: 36466) protocol. Subjects were strapped into a rigid-back chair, and a gentle load was applied to the center of mass of the head through wrestling headgear, inducing sagittal extension (Fig. 1(c)). An in-line tension sensor (TLL-500, Transducer Techniques, Temecula CA) measured the external load applied to the head, sampled at 1500 Hz. To measure head impact kinematics, each subject wore a custom-fit EVA mouthguard rigidly connected to an acrylic bite-bar containing a tri-axis accelerometer (3273A1, Dytran Instruments, Inc., Chatsworth, CA, USA) and three gyroscope s (ARS-PRO-18 K, Diversified Technical Systems, Seal Beach, CA, USA). The bite-bar sensors were triggered to record when the tension sensor read 50 N of force. Kinematics were recorded 100 ms pre-trigger and 500 ms post-trigger. All kinematic sensor data were collected at 10 kHz and low-pass filtered with a fourth-order Butterworth 300 Hz cutoff.

A total of six trials per subject were used to fit stiffness and damping parameters (the six trials in which a standard chinstrap was used). In three trials, subjects were instructed to remain upright and to minimally activate neck muscles. In the other three trials, subjects were instructed to fully co-contract the neck muscles prior to impact. A custom electromyogram system was attached to each subjects' sternocleidomastoid muscle and acquired using an oscilloscope (TDS 2004 B, Tektronix, Santa Clara CA) to measure muscle activity and to validate that subjects were activating their neck muscles appropriately for the given trial. Subjects were warned that an external load would occur within the next 10 seconds. The load was then applied after a random wait of 2–10 seconds to minimize impact anticipation. Test conditions were randomly ordered to prevent habituation.

Detailed methods of this study are further discussed in [27].

C. Parameter Identification and Model Validation

Linear torsional spring dampers were used to represent the combined action of the neck muscles, ligaments, tendons, and other soft tissue loads crossing each joint. For each subject, two sets of joint stiffness and damping values were fit for both the OC and C7 joints, corresponding to minimal and maximal muscle activations. The Matlab genetic algorithm function ("ga"), part of the global optimization toolbox (Mathworks, Waltham, MA), was used to minimize a fitness function which calculated the least squares error between the simulated angular velocity trace and the experimental angular velocity trace over the three activated or relaxed neck muscle trials. The "hybrid function" option was used, so that at the end of the genetic algorithm global optimization, the local minimizer function "patternsearch" was used to ensure convergence to the optimum point. For the springs, the optimizer was constrained to search between 0 and 1000 Nm/rad; for the dampers, between 0 and 30 Nms/rad. Other model parameters, including link lengths and inertial properties, were set to 50% male values [28].

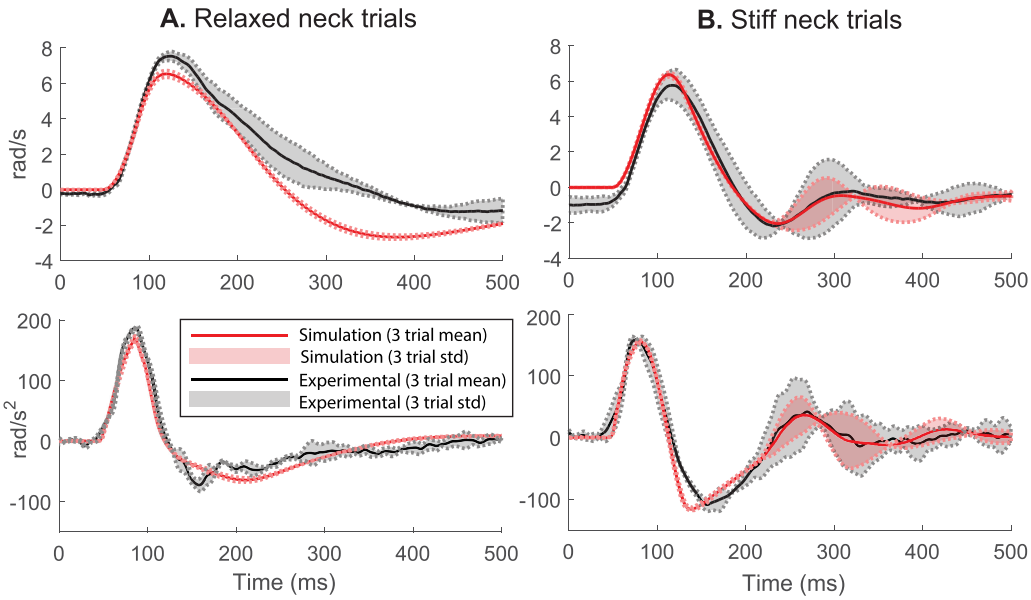

Fig. 2. Model fit to experimental data. Stiffness and damping values of the C7 and OC joints corresponding to minimum and maximum neck muscle activation were fit using human subject data. Shown here are the results from Subject 2. Aggregate results are presented in Table II. The applied load to the head is an approximate half-sine of 60–80 ms duration with an amplitude of 150–200 N, depending on subject and trial number. Load time traces are shown in [27].

TABLE II
SUBJECT-SPECIFIC JOINT PARAMETER VALUES AND VAF

Relaxed trials	Subj. 1	Subj. 2	Subj. 3	Subj. 4	Subj. 5
k_{C7} (Nm/rad)	0.051	1.197	1.696	0.025	4.703
k_{OC}	0.001	0.552	3.786	0.000	16.69
b_{C7} (Nms/rad)	1.941	1.471	2.234	2.059	2.813
b_{OC}	1.140	0.555	1.147	1.107	0.097
VAF (%)	90.6±1.0	80.0±1.7	96.8±1.8	81.6±3.9	89.1±2.
Tensed trials	Subj. 1	Subj. 2	Subj. 3	Subj. 4	Subj. 5
k_{C7} (Nm/rad)	26.11	20.28	13.89	27.15	20.96
k_{OC}	45.82	30.10	10.85	77.87	46.72
b_{C7} (Nms/rad)	2.303	2.854	2.072	1.597	3.52
b_{OC}	5.504	3.048	2.831	5.730	1.571
VAF (%)	89.3±10	89.0±7.9	96.7±0.6	86.9±3.7	93.7±3.

Fig. 2 shows the simulated and experimental angular kinematics corresponding to tensed and relaxed muscles for one of the subjects. Experimental angular acceleration was found by differentiating velocity with a 4th order stencil. To quantify the goodness-of-fit, we calculated the variance accounted for (VAF) by each subject-specific model:

$$VAF = \left(1 - \frac{\sum\left(\dot{\theta}_{exp} - \dot{\theta}_{sim}\right)^2}{\sum \dot{\theta}_{exp}^2}\right) * 100 \qquad (6)$$

Table II shows aggregate stiffness and damping values for the OC and C7 joints for all five subjects, as well as the VAF for each model. A VAF of 100% represents a perfect fit.

D. Force-Rotational Admittance Derivation

Leveraging techniques from the robotics literature on the inertia of manipulators [29], we define and quantify a new term to describe the head's resistance to rotation, which we call "force-rotational admittance" (FRA). The force-rotational admittance is an analytical measure of how much angular acceleration the head will experience from a linear input force at a given point on the skull. It is based entirely on the linkage configuration dependent effective inertial properties of the end-effector, or the head. It is derived by mapping the mass matrix of the system (1) into the coordinate frame of the end-effector using the state-dependent Jacobian.

We refer to the equations of motion outlined in (1), (2), and (3) as the "joint-space" dynamics, representing system dynamics with the generalized coordinates of the joints. The dynamics of the system within the coordinate frame of the end-effector (a point on the head) can be considered the "operational-space" dynamics. The Jacobian matrix, which relates joint velocities to end-effector velocities, maps between joint-space coordinates and operational space coordinates. The "kinetic energy matrix", a measure of the effective inertial properties of the end-effector, can therefore be derived using the mass matrix in joint space (Equation 2) and the Jacobian:

$$\Lambda\left(q\right) = \left(J\left(q\right) M^{-1}\left(q\right) J^{T}\left(q\right)\right)^{-1} \qquad (7)$$

Where q is the matrix of the generalized coordinates in joint space (Table I):

$$q = \left[\theta \ \phi \ x\right] \qquad (8)$$

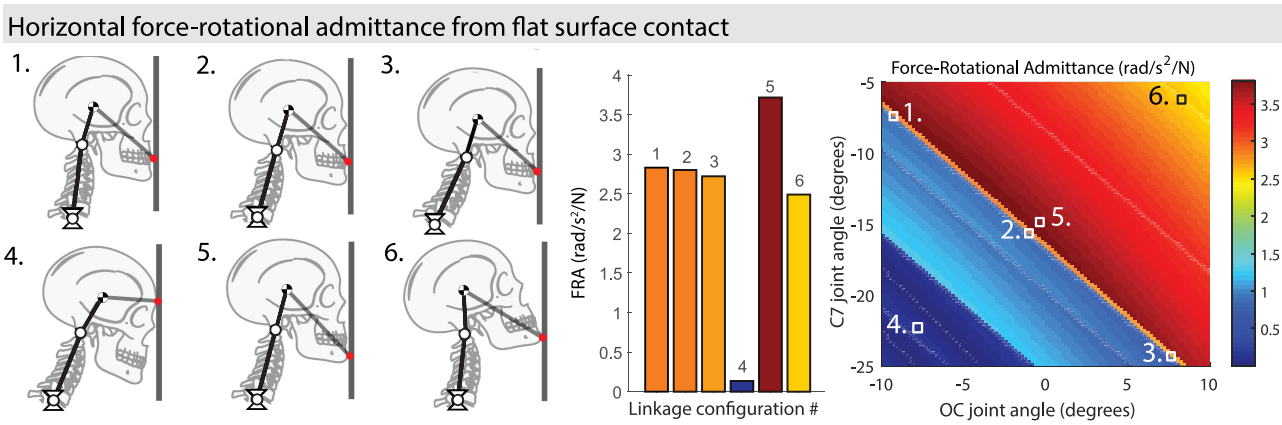

Fig. 3. Force-rotational admittance from flat surface contact. We considered a skull impacting a flat plane in a variety of head-neck linkage configurations over a 20 degree C7 and OC joint range. The FRA was derived at the point on the skull closest to the plane. Six configurations of interest are shown. Both impact location and head striking angle can drastically change the FRA, and therefore the expected head angular acceleration.

The Jacobian matrix associated with the linear velocities of a point on the skull is:

$$J_v = \begin{bmatrix} -L\cos\theta - h\cos(\theta+\phi) - \rho\cos(\theta+\phi+\gamma) & \\ -h\cos(\theta+\phi) - \rho\cos(\theta+\phi+\gamma) & 1 \\ -L\sin\theta - h\sin(\theta+\phi) - \rho\sin(\theta+\phi+\gamma) & \\ -h\sin(\theta+\phi) - \rho\sin(\theta+\phi+\gamma) & 0 \end{bmatrix} \tag{9}$$

The distance and angle between the skull center of mass and impact point are denoted with variables ρ and γ. The Jacobian matrix associated with the angular velocity of the head, for any point on the skull, is:

$$J_w = \begin{bmatrix} 1 & 1 & 0 \end{bmatrix} \tag{10}$$

$\Lambda_{vw}(q)$ describes the coupling between linear input forces and head angular velocities:

$$\Lambda_{vw}(q) = J_v(q) M^{-1}(q) J_w^T(q) \tag{11}$$

M(q) is the mass matrix of the system in joint space as described by Equation 2. Given any input force vector $F = [F_x\ F_y]$ acting through a certain point on the head, the analytical solution to the instantaneous angular acceleration the head will experience from that input force at that point is given by:

$$\alpha_{head} = F \cdot \Lambda_{vw}(q)^T \tag{12}$$

Similarly, the head's linear acceleration response to an input force can be found as follows:

$$\Lambda_v(q) = J_v(q) M^{-1}(q) J_v^T(q) \tag{13}$$

$$\ddot{x}_{head} = \|F \cdot \Lambda_v(q)\|_2 \tag{14}$$

For our analysis, we are interested in the relative susceptibility of the head to angular acceleration at different points on the skull and with different neck joint configurations, generalized to any input force magnitude. Thus, we define the force-rotational admittance (FRA) and force-linear admittance (FLA) as follows:

$$FRA = u \cdot \Lambda_{vw}(q)^T \tag{15}$$

$$FLA = \|u \cdot \Lambda_v(q)\|_2 \tag{16}$$

Vector u is a unit vector describing a force input direction. The FRA (rad/s^2/N) and FLA (m/s^2/N) at a point on the skull give a measure of how much angular and linear acceleration the head will experience from a unit input force.

E. Force-Rotational Admittance at Points on the Human Head

The utility of the FRA in understanding how the head-neck positioning dictates head rotation is visualized in Fig. 3, where we show small changes in head-neck positioning can significantly vary the expected head impact angular acceleration. We considered a skull impacting a flat plane in 1000 different head-neck linkage configurations varying over a 20 degree C7 and OC joint range. In previous studies, the OC joint has been found to have a range of motion up to approximately 20 degrees in flexion-extension [30]. In our two-pivot model, the single C7 pivot represents the remaining T1-C2 vertebrae motion, which cumulatively have a range over 100 degrees in flexion-extension [31]. However, in Fig. 3, we show a C7 joint range of only 20 degrees to match the OC joint range for illustrative purposes. In each configuration, we derived the FRA to a horizontal input force at the "impact point" on the skull closest to the vertical plane, and chose six configurations of interest. From this analysis, we see that the FRA is sensitive to both the impact location and the linkage configuration. Small changes in linkage angles of just a few degrees can change the FRA, and therefore the expected angular acceleration, by orders of magnitude. For example, configuration 5 is only a few degrees different than configuration 4, although the FRA is over an order of magnitude higher. The primary factor in determining the resulting FRA is the orientation of the skull relative to the impact plane. The orientation of the skull is controlled by the C7 and OC joint angles, but different joint angle combinations can lead to the same skull orientation, and therefore the same FRA value. For example, configurations 1, 2, and 3 all have different OC and C7 joint angles, but have almost identical skull orientations relative to the impact force, so the FRA at the point of contact is nearly identical. Conversely, in configurations 5 and 6, the

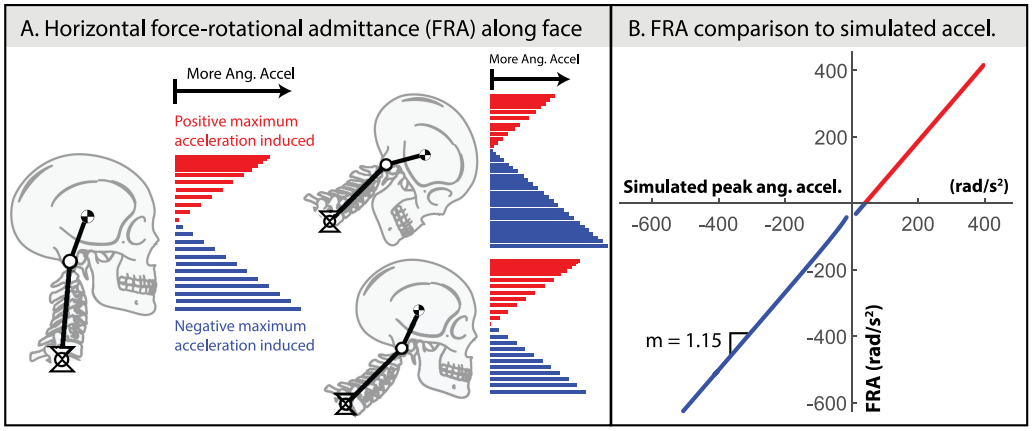

Fig. 4. Force-rotational admittance along skull face. (a) The FRA was derived along the front of the head from a horizontal impact force. The length of each line visualizes how much angular acceleration the head will experience from a force input along that line. (b) The FRA was compared to simulated angular acceleration from 10 ms, 150 N impacts. The simulated peak angular acceleration and the predicted FRA angular acceleration values are correlated with a slope of 1.15, suggesting that changes in FRA correspond closely to changes in peak angular acceleration in fast impacts.

contact point is on the chin, yet the FRA of 6 is much lower due to the different orientation of the skull relative to the impact force. It can be seen in Fig. 3 that there are diagonal "iso-lines" of approximately constant FRA value; these lines correspond to joint configurations that lead to constant skull orientation relative to the impact force. The sharp boundaries along the diagonal represent when the point of contact transitions from the chin up to the forehead.

In a realistic impact scenario, a complexity of forces can act on the skull at various locations, sometimes in quick succession [32], [33]. We extended our analysis in Fig. 4(a), by deriving the FRA to a horizontal input force at points along the length of the skull face. The length of the line represents the FRA magnitude, and the color represents FRA directionality (positive or negative). Based solely on the inertial properties of the head and neck, the angular acceleration response of the head varies significantly in both magnitude and direction. This formulation predicts that there is an optimal contact location on the skull, at which the angular acceleration response will be minimized, which varies in location based on head-neck positioning.

The FRA predicts the angular response of the head to an instantaneous input force. The force from a typical head impact in contact sports, such as football, acts more like a half-sine input over 10–40 ms [25], [34]. Thus, the head-neck configuration at the time of peak force is slightly different than the initial head-neck configuration. To quantify the accuracy of the FRA in predicting peak head angular acceleration from these short-duration impacts, we compared the FRA to the simulated angular head acceleration from a 150 N, 10 ms half sine force at impact points up and down the face of the skull (Fig. 4(b)). We found that changes in peak angular head acceleration correlate to changes in FRA value with a slope of 1.15, demonstrating that comparing the FRA at different impact points gives a good estimate of the relative head angular acceleration experienced.

F. Influence of Muscle Activation on Head Rotation

To understand the effects of increasing soft tissue forces due to muscle activation on head rotation, we subjected our subject-specific head-neck models to a variety of input forces to represent different impact conditions. To best match the impact conditions of our laboratory human subjects, the impact force was applied horizontally at the head center of mass, with the cervical spine in an upright position.

In Fig. 5(a), we applied an impulse of 6 N-s to the head in all five subject-specific models of both tensed and relaxed neck muscles. The impulse was kept constant over different force durations to represent scaling in realistic impact scenarios – in general, shorter and faster head impacts will be higher in force magnitude while longer and slower impacts will be lower. The average reduction in peak angular head kinematics was plotted over different impact durations. At the low impulse severity, full neck muscle activation lowered peak angular head velocity and acceleration by up to 40% in 160 ms impacts, with a lesser effect in shorter duration impacts. Fig. 5(b) simulates a more severe impulse of 50 N-s meant to represent a force input which could cause injury [25]. In impacts with long contact durations of over 100 ms, angular velocity was similarly reduced by nearly 30% from minimum to maximum muscle activation; however, in the region that football head impacts are most likely to fall under, between 10–40 ms, a ngular velocity was only reduced by 10–20%. In both low and high severity impulses, head angular acceleration increased with increased muscle activation in very short duration impacts of less than 15 ms.

Example angular acceleration traces from three different impacts, with varying levels of muscle activation, are shown in Fig. 5(c), (d), (e) using the head-neck model of Subject 1. In a 150 N impact of 65 ms, muscle activation reduced kinematics by 15% (Fig. 5(c)). In a 3000 N impact of 25 ms, angular acceleration was only reduced 3%. In a 500 N impact of 150 ms duration, the first peak in angular acceleration was reduced by over 30%.

G. Force-Rotational Admittance of the Woodpecker

In humans, we found that the analytically-derived FRA, based purely on head-neck inertial and geometric properties, can accurately predict how much angular acceleration the head will

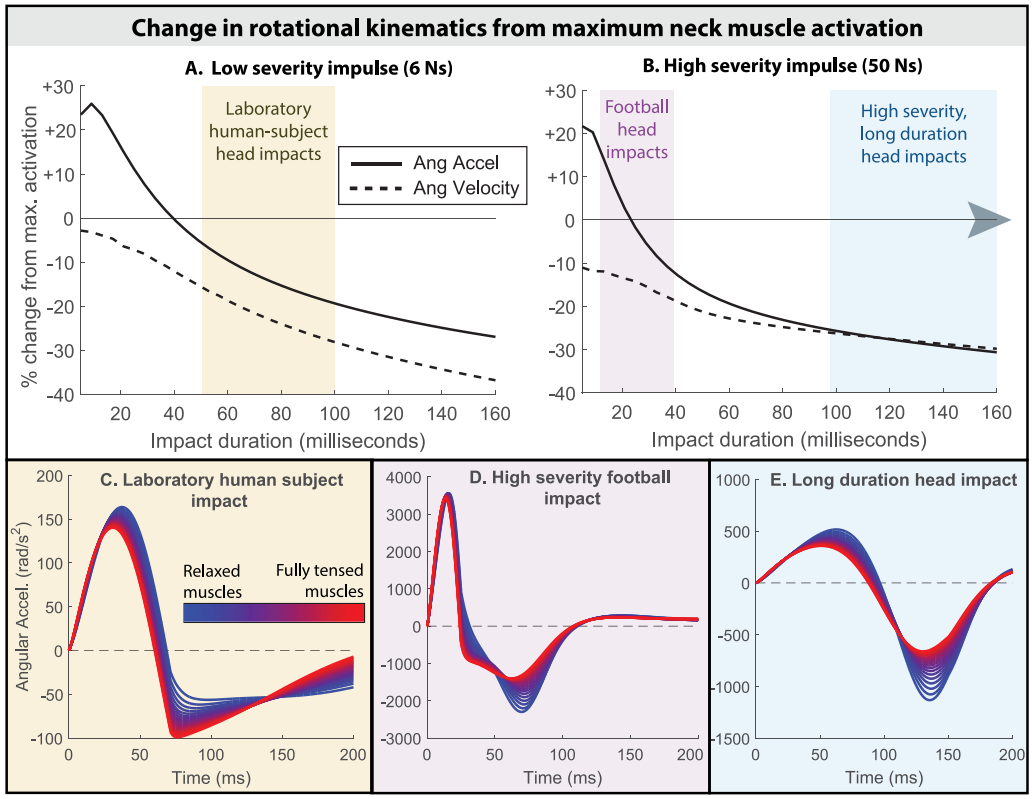

Fig. 5. The effect of muscle activation on head kinematics. Relative to the positioning of the head and neck, the soft tissue has a lesser effect on head impact rotation. (a) A low severity impulse of 6 N-s and (b) A high severity impulse of 50 N-s was applied to the center of mass of the head to each subject-specific model to represent the laboratory testing. Averaging over all five subjects, the reduction in angular acceleration and velocity over different impact durations was plotted. We plotted the simulated traces of (c) laboratory head impacts, (d) high speed football impacts, and (e) longer duration head impacts at various levels of muscle activation. The red trace represents the stiffness and damping values that correspond to full muscle activation, while the blue trace represents the values corresponding to relaxed muscles. To represent partial muscle activation, stiffness and damping parameters were linearly interpolated between minimum and maximum muscle activation values and are shown as a gradient varying from blue to red.

experience from a short duration input force. Conversely, soft tissue forces had a relatively insignificant effect. Woodpeckers experience linear head accelerations of up to 1000 g over 1–2 ms [3]; however, the rotational component of these accelerations remain unknown. Because deriving the FRA requires no information about soft tissue properties, we can estimate the woodpecker head impact rotation from the short duration impacts it experiences based solely on its hard skeletal tissue anatomy.

We modified our two-pivot head-neck human model to approximately match the geometric and inertial properties of the woodpecker (Table III). Link lengths and joint locations for the woodpecker model were taken from a CT scan of a whole body *Picoides albolarvatus* [35], taken from the NSF digital library. CT scan slice data were uploaded into Fiji image processing package. The torso was assumed to be fixed to model the bird perched on a tree. Lengths and geometries were extracted using Fiji. Mass and inertia properties were taken from previously published values [36]. The angle of the woodpecker's beak at time of contact was characterized in a previous study to be roughly 79 degrees below horizontal [37]. Knowing this contact angle, and the geometric link lengths of the beak, head, and cervical spine, we estimated the upper and lower cervical spine joint angles of the woodpecker at contact, shown as configuration 3 in Fig. 6.

TABLE III
WOODPECKER LINKAGE MODEL SYMBOLS AND PARAMETER VALUES

Symbol	Quantity	Value	Source
m_H	Head mass	0.009 kg	[32]
m_B	Body mass	0.06 kg	[32]
m_N	Neck mass	0 kg	Estimated
L	Lower linkage length	0.025 m	[31]
h	Upper linkage length	0.0108 m	[31]
L_{beak}	Head CoM to beak tip	0.03 m	[31]
H_{zz}	Head moment of inertia	1.25e-4 kgm^2	[32]
N_{zz}	Neck moment of inertia	0 kgm^2	Estimated

To match a typical woodpecker pecking force, the FRA of a horizontal impact force at the tip of the woodpecker beak was analyzed over a 40 degree range of upper and lower joint values (Fig. 6). At configuration 3, our estimated pre-impact linkage configuration, the derived FRA is near minimum, suggesting that woodpeckers position their head and neck, relative to the impact force, in a way which minimizes head rotation, despite experiencing severe linear accelerations. Configurations 2 and 4

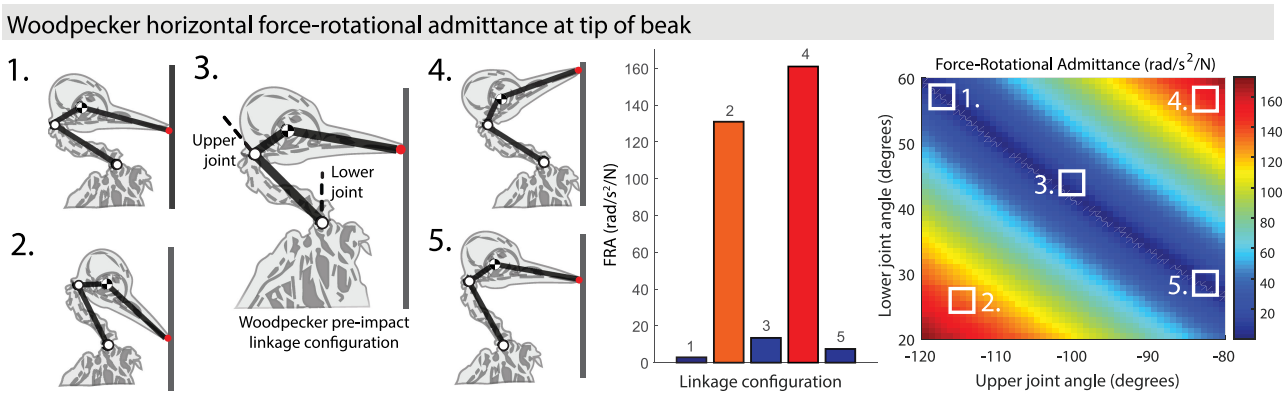

Fig. 6. Force-rotational admittance of a woodpecker. We adapted our linkage model to match the geometry and inertia of a woodpecker. We considered a woodpecker impacting a flat plane in a variety of head-neck linkage configurations over a 40 degree lower and upper joint range, and derived the FRA to a horizontal force at the beak tip. Five configurations of interest are shown. Configuration 3 corresponds to the estimated positioning of a woodpecker prior to impact; this corresponds to a near minimum FRA value.

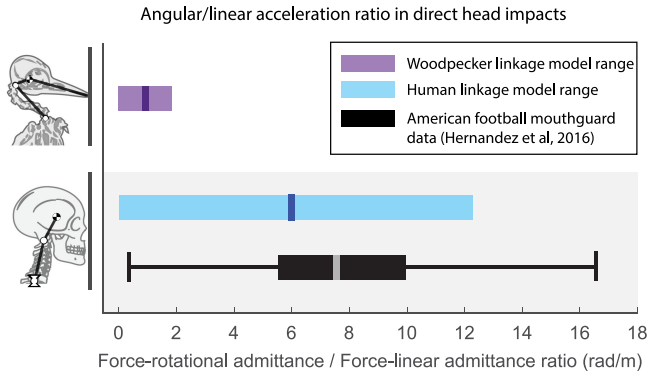

Fig. 7. Angular/linear acceleration ratio in woodpeckers and humans. We divided the force-rotational acceleration (expected angular acceleration) by the force-linear acceleration (expected linear acceleration) in woodpeckers, shown in purple, and humans, shown in blue. We also compared 421 in-vivo human head impacts recorded with an instrumented mouthguard in American football. Woodpeckers experience far less relative angular to linear head acceleration.

would result in angular accelerations nearly an order of magnitude higher. Interestingly, configurations 1 and 5 have a similar FRA to configuration 3, as they lead to a similar head striking position.

The difference in relative linear to angular accelerations between humans and woodpeckers is further explored in Fig. 7. The analytically-derived rotational response of the head (FRA) was divided by the linear acceleration response of the head (FLA) to quantify the relative angular-linear acceleration experienced from a horizontal impact force. From a force applied at the tip of the beak, the woodpecker experiences a ratio up to 1.84 rad/m at ± 20 degrees about its nominal pre-impact linkage configuration. Conversely, a human can experience forces anywhere on the head. Over the cervical spine joint limits of a human, our model predicts they can experience a ratio up to 12.27 rad/m from a horizontal impact with a surface.

In-vivo data supports model results. Taking 421 American football direct head impacts captured with an instrumented mouthguard [34], the vast majority of these impacts had a peak angular to linear head acceleration ratio between 5.8 and 10 rad/m, with a few outliers up to 17 rad/m, far above that of our woodpecker model. The small discrepancy between our model and human data may be due to the modeled torso being constrained to translation only.

III. Discussion

Using a simplified rigid linkage model of the head and neck, we found that small changes in head-neck positioning can drastically change the effective admittance of the head to rotation, and can change peak angular head accelerations by orders of magnitude. Comparatively, the soft tissue loads from increasing muscle activation from minimum to maximum values had a much lesser effect, which varied based on impact scenario.

A. Two-Pivot Rigid Linkage Manipulator Model

In a previous study, the authors found that, in sagittal extension, the head instantaneous center of rotation moves significantly up and down the length of the neck, and thus a multi-joint system must be used to properly capture its motion [27]. Anatomically, this may be due to the compliance of the neck at the atlanto-occipital joint, which allows bending in sagittal flexion but not lateral extension. From the perspective of the head as a robotic "end-effector" of the cervical spine, utilizing a two-pivot model is also fitting. In the sagittal plane, a human can actively rotate their head by bending their lower cervical spine, while independently nodding their head about the atlanto-occipital joint. Thus, two rotational degrees of freedom are needed to describe how the cervical spine controls rotation of the head relative to the torso. Even complex rigid-body models of the cervical spine use only two rotational degrees of freedom in sagittal extension; for example, in [38], the bending of the lower joint is distributed over the C2-C7 vertebrae, while the C1 vertebrae is given the freedom to rotate independently.

In this study, we showed that a two-pivot model can accurately capture the sagittal plane head kinematics of human head impacts with proper stiffness and damping values fit to each joint. Table II overviews the stiffness and damping values fit to each subject. Joint stiffness and damping varied considerably across

subjects, but increasing muscle activation generally increased both stiffness and damping across all subjects, as expected. The neck joint parameter values found in this study are similar to those of similar previous studies which treated the neck as a single pivot joint. In [12], it was found that the average neck stiffness varied between 14 and 22 Nm/rad in sagittal extension, while average viscosity varied between 1.8 and 2.4 Nm-s/rad. In [14], average stiffness was found to vary between 22.6 and 41.3 Nm/rad. The larger range found in the present study likely reflects the more significant differences in exertion level that was instructed to the test subjects. A large stiffness range was found in [39], [40], between 28.4 up to nearly 300 Nm/rad, with varying levels of neck muscle activation. The authors in these studies neglected damping and considered the dynamic stiffness rather than the static stiffness, which likely accounts for this increased range.

Similar to prior studies [12], [39]–[41], we found a large variance in stiffness parameters between subjects and muscle activation levels. We expect this variance to be in part due to differences between subjects in active muscle strength, passive muscle fiber properties, and geometric properties such as muscle moment arms and attachment points. Many neck muscles span multiple joints in the neck, and have considerable variation in number and location of tendon attachment points between individuals [42]. It is conceivable that neck joint parameters could vary significantly between subjects depending on these factors.

Two-pivot neck models have been used extensively to capture the global kinematics of human subjects in whiplash tests in a series of studies from the Navy in the 1970's and 1980's [43]. Although the method of head loading in these trials came from torso accelerations, fundamentally different than the direct head loading in this study, the stiffness and damping values used to fit this data fall within the range of values found using our methodology. This suggests that human neck stiffness and damping parameters may stay consistent over different methods of head loading and impact durations.

B. Head-Neck Positioning Dictates Rotational Impact Kinematics

Our simple linkage model allows us to derive analytical relationships between the head positioning and its rotational response to an input force, which we termed the force-rotational admittance (FRA). The FRA predicts that small changes in head-neck positioning can change head angular acceleration by orders of magnitude by changing the effective end-effector inertia. This effect is far greater than the effect of increasing soft tissue forces to maximal muscle activation. This signifies the importance of proper head positioning prior to impact, and helps to explain the underlying mechanisms behind the clinically observed relationships between head orientations and resulting accelerations [25].

Our FRA analysis shows there is an optimal contact location on the skull from a horizontal input force (Fig. 4). This location varies in height depending on the configuration of the neck joints. Although the relationship between the vertical impact location, neck joint angles, and resulting FRA is mathematically complex, in general, forces further from the center of mass of the head resulted in higher FRA values and head angular accelerations. Indeed, past experimental studies have found that non-centric impacts, or "glancing blows," can lead to significantly larger head angular accelerations than centric impacts [44], [45].

The results from this work have noteworthy implications on the design of helmets and other protective gear. The FRA can be used as a tool to evaluate how placing an object on the head will effect rotational head accelerations. For example, we found that the head has a higher FRA to a horizontal input force on the chin than on the forehead; this trend would likely be amplified with a football helmet facemask, which protrudes out further than the chin. Likewise, the FRA could be used to quantify how protrusions on the forehead, such bicycle helmet visors, affect angular accelerations in frontal impacts. It is important to consider how protective gear add-ons affect the head's vulnerability to angular accelerations, and in future work the FRA can be used to optimize the shape and geometry of protective gear to minimize head rotation. Similarly, this approach could be used to suggest rule changes that enforce proper head positioning prior to tackling in contact sports.

Lastly, we showcased the utility of the FRA by studying the inertial properties of the woodpecker, an animal which experiences linear accelerations orders of magnitude above concussive-level human head accelerations without apparent injury [3], [37]. We found that the woodpecker linkage configuration at impact naturally occurs near a minimum of the FRA from a horizontal input force. We posit that this could contribute to their brain injury resilience; given the rapidly-increasing body of evidence that head rotation is a key factor in TBI in humans [9], [46], it can be reasonably assumed that woodpeckers, by reducing head rotation, are lowering their risk of brain injury. Indeed, a previous high-speed video analysis of woodpecker impacts found that the beak trajectory is nearly linear before and after impact [3]. It is important to emphasize that this could be one of many reasons why woodpeckers are more resilient to brain injury. Many studies have presented a number of theories about the unique shape and energy absorption properties of skull and hyoid apparatus of the woodpecker [47]–[50]. Others have suggested that brain tolerance to acceleration is inversely related to brain mass; a woodpecker's brain mass is roughly 0.1–0.5% that of a human, making it far more tolerant to both linear and angular acceleration [3], [37], [51]. Our results suggest that the positioning of their skeletal tissue may contribute to these other mechanisms to help explain how brain injury is avoided. With the proper anatomical and inertial properties, this approach could be used to study the head impact rotation of other animals resilient to brain trauma, such as the bighorn sheep.

C. The Effects of Neck Muscle Activation Vary Based on Impact Scenario

Through simulations of different head impact durations and severities, we found that increasing the soft tissue forces from

fully activating the neck muscles had a different effect in different impact scenarios. This could help to explain much of the conflict in currently literature about the link between neck strength or activation and injury risk.

Due to ethics considerations, it is not possible to obtain human subject data from injury-level head impacts in laboratory testing. Thus, laboratory head impact tests involving human subjects typically employ low severity impacts of long duration (between 50–100 ms) and try to extrapolate to higher severities. In this lower severity impact regime, our models predicted that fully activating the neck muscles reduces peak angular head accelerations by up to 20% and velocities by up to 30%, when averaged over the 5 subjects. This is in line with other similar experimental studies: [15] found that anticipatory activation reduced peak angular velocity on average by 9.6%; [12] found that activation reduced peak angular velocity by 18.6%; and [14] found that anticipation reduced peak angular acceleration by 25% in male subjects. These studies postulated that muscle activation can reduce the risk of injury, yet our model showed that increasing soft tissue forces has a different effect in high severity impact scenarios.

In short duration, high severity impacts, similar to what could be experienced in contact sports, our models predicted that fully activating the neck muscles had a lesser effect on reducing angular velocity. Further, we found that in very short duration impacts below 20 ms, angular accelerations increased from activating neck muscles. Although this result was unexpected, it is in line with other work which utilized more complex finite element models. In finite element simulations of short duration head impacts in a variety of contact sports, it was found that muscle activation increased angular accelerations in a majority of the trials; the authors attributed this increase to muscle activation changing in the effective center of rotation of the head [22]. Similarly, a finite element study of pedestrian impacts found that there was an increase in brain tissue strain by up 1–14% due to muscle activation [23]; presumably, this tissue strain is correlated with rotational acceleration.

These results suggest that soft tissue forces are incapable of substantially reducing the angular kinematics in head impacts when compared to the head-neck positioning. This result may help to explain the field studies that did not find reductions in peak head accelerations due to increases in static strength or muscle activation of the neck, despite their initial hypotheses that predict otherwise [18]–[20]. Because of the small effect of the soft tissue on rotational kinematics, the effect of increasing neck stiffness and damping due to muscle activation or strengthening may be statistically undetectable without a substantially large number of impact trials, which are not logistically possible or safe in an in-vivo human study.

It has been argued that neck muscle activation can reduce angular velocity from concussive-level impacts in the coronal plane by reducing angular velocity by 22% [21]. However, in lateral flexion, the neck acts more like a single pivot joint [27], and thus the effects of soft tissue forces likely vary in this plane from what we found with our sagittal plane model. Regardless, the reduction found in [21] is still relatively insignificant compared to that of head-neck positioning found in the present study.

D. Study Limitations and Future Work

The primarily limitation of this study is that the model developed is a simplification of human anatomy. We are using a two-dimensional lumped parameter model of the cervical spine, whereas the human neck is much more complex, with highly non-linear stiffness and damping values which likely vary greatly between subjects. It has been shown that the neck joints become much stiffer as they reach their joint limits [41], [52]. Due to safety reasons, we were unable to test human subjects near these joint limits, and it is unknown how the stiffness and damping values change in these limits with increased muscle activation. Thus, our soft tissue results only remain valid as long as the neck remains within its joint limits, where stiffness and damping is more linear. Further, the cervical spine has some axial compliance and can buckle under large loads [53], which was neglected in this study, and may affect the derived head inertial properties. Additionally, the model was based on data from only five male subjects, who may not be representative of the general population; the average physiology differed slightly from that of the 50th percentile male [27]. As such, the findings from our model represent high-level trends and estimates rather than comprehensive conclusions. In future work, a more anatomically detailed model could further elucidate how neck parameters vary with muscle activation or strength, and quantify the contribution from different soft tissue structures. A more complex model would also allow a comprehensive study on how head-neck positioning affects the tradeoff between brain and neck injury risk, as we did not investigate how head positioning affects the risk of cervical spine injury, which is known to be sensitive to impact orientation [24], [54]. Additionally, the FRA quantifies head angular acceleration, which has been found to be correlated to injury risk. However, the relationship between head rotation, brain tissue strain, and resulting neurological outcome is still under investigation. Future brain injury studies may uncover the importance of linear motion in brain injury, which was assumed to be safer than angular motion in this study. Lastly, this model only investigated sagittal plane impacts. The cervical spine is known to constrain the head differently in different planes of motion [27], which could lead to different results in the effect of both hard and soft tissue.

Future human subject studies are needed to verify the physiological relationships found in this paper. The experimental protocol used in the present study could be adapted to different loading magnitudes and durations (within safe limits), non-centric head loading, and different loading directions (e.g., off-axis loading) to verify the hypotheses generated by our rigid-linkage model and provide insight into its limitations. This study could also guide the development of biofidelic surrogate neck models, which could be used to experimentally validate our FRA results.

IV. Conclusion

Here, we present a rigid linkage manipulator model of the head and neck using laboratory human subject data to study the effect of the head-neck positioning versus the soft tissue forces on head impact rotation. We introduced the "force-rotational admittance," an analytical solution to the rotational response of the head from an input force at a certain point. Our models demonstrated that small changes in head-neck positioning can affect the rotational response of the head by an order of magnitude. Comparatively, increasing soft tissue forces from full neck muscle activation had a lesser effect, which depended on the contact duration and severity.

The simple rigid linkage models presented in this work provide clear, meaningful insights and analytical solutions to high-level trends that would be confounded with more complex models. Our FRA analysis, based purely on geometric and inertial properties, can be used to study the head rotation in other animals, and to drive the development of protective gear meant to minimize head rotations.

Acknowledgment

The authors would like to thank M. Kurt and K. Laksari for their help with dynamic modeling, L. Wu for her help with running and analyzing simulations, and H. Alizadeh for insightful discussions about optimization.

References

[1] O. Khatib *et al.*, "Robotics-based synthesis of human motion," *J. Physiol. Paris*, vol. 103, nos. 3–5, pp. 211–219, 2009.
[2] E. Demircan *et al.*, "Muscular effort for the characterization of human postural behaviors," *Springer Tracts Adv. Robot.*, vol. 109, pp. 685–696, 2016.
[3] P. R. A. May *et al.*, "Woodpecker drilling behavior: An endorsement of the rotational theory of impact brain injury," *Arch. Neurol.*, vol. 36, no. 6, pp. 370–373, 1979.
[4] A. Drake *et al.*, "Horn and horn core trabecular bone of bighorn sheep rams absorbs impact energy and reduces brain cavity accelerations during high impact ramming of the skull," *Acta Biomater.*, vol. 44, pp. 41–50, 2016.
[5] K. M. Guskiewicz *et al.*, "Association between recurrent concussion and late-life cognitive impairment in retired professional football players," *Neurosurgery*, vol. 57, no. 4, pp. 719–726, 2005.
[6] A. H. S. Holbourn, "Mechanics of head injuries," *Lancet*, vol. 242, no. 6267, pp. 438–441, 1943.
[7] T. A. Gennarelli *et al.*, "Diffuse axonal Injury: An important form of traumatic brain damage," *Neuroscientist*, vol. 4, no. 3, pp. 202–215, 1998.
[8] A. K. Ommaya *et al.*, "Cerebral concussion in the monkey: An experimental model," *Science*, vol. 153, no. 3732, pp. 211–212, 1966.
[9] S. Kleiven, "Predictors for traumatic brain injuries evaluated through accident reconstructions," *Stapp Car Crash J.*, vol. 51, pp. 81–114, Oct. 2007.
[10] C. Hrysomallis, "Neck muscular strength, training, performance and sport injury risk: A review," *Sports Med.*, vol. 46, no. 8, pp. 1111–1124, 2016.
[11] J. D. Schmidt *et al.*, "The influence of cervical muscle characteristics on head impact biomechanics in football," *Amer. J. Sports Med.*, vol. 42, pp. 2056–2066, 2014.
[12] M. Simoneau *et al.*, "Role of loading on head stability and effective neck stiffness and viscosity," *J. Biomech.*, vol. 41, no. 10, pp. 2097–2103, 2008.
[13] C. L. Collins *et al.*, "Neck strength: A protective factor reducing risk for concussion in high school sports," *J. Primary Prev.*, vol. 35, no. 5, pp. 309–319, 2014.
[14] R. T. Tierney *et al.*, "Gender differences in head-neck segmnet dynamic stabilization during head accelaration," *Med. Sci. Sports Exerc.*, vol. 37, no. 2, pp. 272–279, 2005.
[15] J. T. Eckner *et al.*, "Effect of neck muscle strength and anticipatory cervical muscle activation on the kinematic response of the head to impulsive loads," *Amer. J. Sports Med.*, vol. 42, no. 3, pp. 566–576, 2014.
[16] G. M. Gutierrez *et al.*, "The relationship between impact force, neck strength, and neurocognitive performance in soccer heading in adolescent females," *Pediatr. Exerc. Sci.*, vol. 26, no. 1, pp. 33–40, 2014.
[17] K. Hasegawa *et al.*, "Does clenching reduce indirect head acceleration during rugby contact?" *Dental Traumatol.*, vol. 30, no. 4, pp. 259–264, 2014.
[18] P. Lisman *et al.*, "Investigation of the effects of cervical strength training on neck strength, EMG, and head kinematics during a football tackle," *Int. J. Sports Sci. Eng.*, vol. 6, no. 3, pp. 131–140, 2012.
[19] J. Mansell *et al.*, "Resistance training and head-neck segment dynamic stabilization in male and female collegiate soccer players," *J. Athletic Train.*, vol. 40, no. 4, pp. 310–319, 2005.
[20] J. P. Mihalik *et al.*, "Does cervical muscle strength in youth ice hockey players affect head impact biomechanics?" *Clin. J. Sport Med.*, vol. 21, no. 5, pp. 416–421, Sep. 2011.
[21] X. Jin *et al.*, "The role of neck muscle activities on the risk of mild traumatic brain injury in American football," *J. Biomech. Eng.*, vol. 139, 2017.
[22] C. P. Eckersley *et al.*, "Effect of neck musculature on head kinematic response following blunt impact Christopher," in *Proc. IRCOBI Conf.*, 2017, pp. 674–676.
[23] V. S. Alvarez *et al.*, "The influence of neck muscle tonus and posture on brain tissue strain in pedestrian head impacts," *Stapp Car Crash J.*, vol. 58, pp. 63–101, Nov. 2014.
[24] J. F. Heck *et al.*, "National athletic trainers' association position statement: Head-down contact and spearing in tackle football," *J. Athletic Train.*, vol. 39, no. 1, pp. 101–111, 2004.
[25] D. C. Viano and E. J. Pellman, "Concussion in professional football: Biomechanics of the striking player—Part 8," *Neurosurgery*, vol. 56, no. 2, pp. 266–280, 2005.
[26] M. de Jager, "Mathematical modelling of the human cervical spine: A survey of the literature," in *Proc. IRCOBI Conf. Biomech. Impacts*, 1993, pp. 213–227.
[27] C. Kuo *et al.*, "Spinal constraint modulates head instantaneous center of rotation and dictates head angular motion," *J. Biomech.*, 2018.
[28] N. Yoganandan *et al.*, "Physical properties of the human head: Mass, center of gravity and moment of inertia," *J. Biomech.*, vol. 42, no. 9, pp. 1177–1192, Jun. 2009.
[29] O. Khatib, "Inertial properties in robotic manipulation: An object-level framework," *Int. J. Rob. Res.*, vol. 14, no. 1, pp. 19–36, 1995.
[30] N. Bogduk and S. Mercer, "Biomechanics of the cervical spine. I: Normal kinematics," *Clin. Biomech.*, vol. 15, no. 9, pp. 633–648, 2000.
[31] R. W. Nightingale *et al.*, "Comparative strengths and structural properties of the upper and lower cervical spine in flexion and extension," *J. Biomech.*, vol. 35, no. 6, pp. 725–732, 2002.
[32] F. Hernandez *et al.*, "Six degree-of-freedom measurements of human mild traumatic brain injury," *Ann. Biomed. Eng.*, vol. 43, no. 8, pp. 1918–1934, 2015.
[33] B. M. Knowles *et al.*, "Influence of rapidly successive head impacts on brain strain in the vicinity of bridging veins," *J. Biomech.*, vol. 59, pp. 59–70, 2017.
[34] F. Hernandez *et al.*, "Evaluation of a laboratory model of human head impact biomechanics," *J. Biomech.*, vol. 48, no. 12, pp. 3469–3477, 2015.
[35] D. Staff, "Picoides albolarvatus," 2011.
[36] J. F. V Vincent *et al.*, "A woodpecker hammer," *Proc. Inst. Mech. Eng., Part C, J. Mech. Eng. Sci.*, vol. 221, no. 10, pp. 1141–1147, 2007.
[37] Y. Liu *et al.*, "A study of woodpecker's pecking process and the impact response of its brain," *Int. J. Impact Eng.*, vol. 108, pp. 263–271, 2017.
[38] A. N. Vasavada *et al.*, "Influence of muscle morphometry and moment arms on the moment-generating capacity of human neck muscles," *Spine*, vol. 23, no. 4, pp. 412–422, 1998.
[39] R. Portero *et al.*, "Influence of cervical muscle fatigue on musculo-tendinous stiffness of the head-neck segment during cervical flexion," *PLoS One*, vol. 10, no. 9, p. e0139333, 2015.
[40] R. Portero *et al.*, "Musculo-tendinous stiffness of head-neck segment in the sagittal plane: An optimization approach for modeling the cervical spine as a single-joint system," *J. Biomech.*, vol. 46, no. 5, pp. 925–930, 2013.
[41] S. M. McGill *et al.*, "Passive stiffness of the human neck in flexion, extension, and lateral bending," *Clin. Biomech.*, vol. 9, no. 3, pp. 193–198, May 1994.

[42] L. K. Kamibayashi and F. J. R. Richmond, "Morphometry of human neck muscles," *Spine*, vol. 23, no. 12, pp. 1314–1323, 1998.
[43] A. C. Bosio and B. M. Bowman, "Simulation of head-neck dynamic response in −Gx and +Gy," in *Proc. 30th Stapp Car Crash Conf.*, 1986.
[44] B. S. Elkin *et al.*, "Brain tissue strains vary with head impact location: A possible explanation for increased concussion risk in struck versus striking football players," *Clin. Biomech.*, Mar. 2018.
[45] A. Post *et al.*, "IRC-12-52 IRCOBI conference 2012," in *Proc. Int. Conf. Res. Council Biomech. Injury*, 2012, pp. 419–429.
[46] S. Ji *et al.*, "Head impact accelerations for brain strain-related responses in contact sports: A model-based investigation," *Biomech. Model. Mechanobiol.*, vol. 13, no. 5, pp. 1121–1136, 2014.
[47] Y. Liu *et al.*, "Response of woodpecker's head during pecking process simulated by material point method," *PLoS One*, vol. 10, no. 4, p. e0122677, 2015.
[48] J.-Y. Jung *et al.*, "Structural analysis of the tongue and hyoid apparatus in a woodpecker," *Acta Biomater.*, vol. 37, pp. 1–13, 2016.
[49] S.-H. Yoon and S. Park, "A mechanical analysis of woodpecker drumming and its application to shock-absorbing systems," *Bioinspir. Biomim.*, vol. 6, no. 1, p. 16003, 2011.
[50] Z. Zhu *et al.*, "Energy conversion in woodpecker on successive peckings and its role on anti-shock protection of brain," *Sci. China Technol. Sci.*, vol. 57, no. 7, pp. 1269–1275, 2014.
[51] L. J. Gibson, "Woodpecker pecking: How woodpeckers avoid brain injury," *J. Zool.*, vol. 270, no. 3, pp. 462–465, 2006.
[52] H. Mertz and L. Patrick, "Strength and response of the human neck," in *Proc. Stapp Car Crash Conf.*, 1971, pp. 2903–2928.
[53] M. Shea *et al.*, "Variations of stiffness and strength along the human cervical spine," *J. Biomech.*, vol. 24, no. 2, pp. 95–107, 1991.
[54] R. W. Nightingale *et al.*, "Impact responses of the cervical spine: A computational study of the effects of muscle activity, torso constraint, and pre-flexion," *J. Biomech.*, vol. 49, no. 4, pp. 558–564, 2016.